Journal of Statistical Physics, Vol. 59, Nos. 5/6, 1990

Low-Viscosity Lattice Gases

B. Dubrulle,[1,2] U. Frisch,[3] M. Hénon,[3] and J.-P. Rivet[3,4]

Received October 11, 1989; revision received December 19, 1989

A class of lattice gas models are studied which are variants of the FCHC model. The aim is to achieve the highest possible Reynolds coefficient (inverse dimensionless viscosity) for efficient simulations of the three-dimensional incompressible Navier–Stokes equations. The models include an arbitrary number of rest particles and violation of semi-detailed balance. Within the framework of the Boltzmann approximation exact expressions are obtained for the Reynolds coefficients. The minimization of the viscosity is done by solving a Hitchcock-type optimization problem for the fine tuning of the collision rules. When the number of rest particles exceeds one, there is a range of densities at which the viscosity takes negative values. Various optimal models with up to 26 bits per node have been implemented on a CRAY-2 and their true transport coefficients have been measured with good accuracy. Fairly large discrepancies with Boltzmann values are observed when semi-detailed balance is violated; in particular, no negative viscosity is obtained. Still, the best model has a Reynolds coefficient of 13.5, twice that of the best previously implemented model, and thus is about 16 times more efficient computationally. Suggestions are made for further improvements. It is proposed to use models with very high Reynolds coefficients for sub-grid-scale modeling of turbulent flows.

KEY WORDS: Lattice gases; transport coefficients; hydrodynamics; computational fluid dynamics.

1. INTRODUCTION

Hydrodynamics is concerned with the large universality class of fluids behaving macroscopically like liquid water. That is to say, their flow at

[1] Observatoire Midi-Pyrénées, 31400 Toulouse, France.
[2] École Normale Supérieure, 75005 Paris, France.
[3] CNRS, Observatoire de Nice, 06003 Nice Cedex, France.
[4] Laboratoire de Physique Statistique, 75231 Paris Cedex 05, France.

0022-4715/90/0600-1187$06.00/0

822/59/5-6-7

velocities small compared to the speed of sound (low Mach numbers) is governed by the incompressible Navier–Stokes equations:

$$\partial_t \mathbf{u} + \mathbf{u} \cdot \nabla \mathbf{u} = -\nabla p + \nu \nabla^2 \mathbf{u} \tag{1}$$

$$\nabla \cdot \boldsymbol{u} = 0 \tag{2}$$

Within this universality class a similarity principle applies: flows in the presence of boundaries of similar shapes have identical (dimensionless) properties, provided they have identical Reynolds numbers:

$$R = LV/\nu \tag{3}$$

Here, ν is the kinematic viscosity of the fluid, a function only of its microscopic structure and of the thermodynamic variables (density, temperature, etc.) and L and V are characteristic scales and velocities of the flows.

The universality class of hydrodynamics contains, in addition to "natural" substances such as air, water, and liquid metals, various artificial *lattice gas* models.[1] The latter are discrete Boolean models governed by deterministic or nondeterministic cellular automata rules, generalizations of the HPP model.[2] Lattice gas models have conservation rules (of mass, momentum, and energy) built into their collision laws. They do not possess the continuous symmetries, e.g., rotational invariance, of the Navier–Stokes equations. Instead, they have only a discrete crystallographic invariance group. If this group is large enough, in particular to ensure the isotropy of fourth-order invariant tensors, then the "macrodynamical" equations of such lattice gases differ from the Navier–Stokes equations by additional terms which become irrelevant in the limit of low Knudsen numbers (scales large compared to mean free path) and low Mach numbers.[3,4] The macrodynamical equations involve also a "Galilean factor" $g(d)$ in front of the nonlinear term $\mathbf{u} \cdot \nabla \mathbf{u}$. It is a function of the (reduced) density d of particles per node and per velocity. Its presence reflects the lack of Galilean invariance at the microscopic level. In the low-Mach-number limit, density fluctuations become irrelevant everywhere (except in the pressure term); this factor becomes constant and may be rescaled out, so that exact Navier–Stokes dynamics is asymptotically recovered, as now confirmed by numerous simulations (see, e.g., ref. 5).

The construction of *three-dimensional* lattice gas models had originally to circumvent the absence of suitable crystallographic groups in three dimensions. This was done by a temporary detour through the fourth dimension, leading to the FCHC lattice.[6] Three-dimensional models will be central to the present paper.

A measure of the efficiency of a lattice gas *model* (prescription of a lattice and of a set of collision rules) for simulating the Navier–Stokes equations is the *Reynolds coefficient* $R_*^{\max}$. It was originally defined in refs. 3 and 7 for the case without rest particles; a more general definition is given in Section 5.4. Roughly, the Reynolds coefficient measures the inverse viscosity in lattice units. For the simulation of a three-dimensional flow with prescribed geometry at prescribed Reynolds and Mach numbers, the computational efficiency is proportional to the fourth power of the Reynolds coefficient. In two dimensions it is the third power.

Achieving the highest possible Reynolds coefficients is important in at least two respects: (i) it allows the numerical simulation of higher Reynolds numbers; (ii) it increases the speed of the computation and/or decreases its cost. Such questions may be of particular relevance in designing optimal three-dimensional special-purpose machines operating by lattice gas algorithms.

It is our purpose here to show how it is possible to systematically improve existing models to achieve higher efficiency. Before outlining the paper, we present an overview of the FCHC models developed so far and the key technical motivations of the present study.

1.1. History of FCHC Models

In the quest for increasingly efficient lattice gas models, our group has by now considered a number of variations of the FCHC model. In order to facilitate reference, we will assign short names to the main models. Table I defines the names and summarizes the properties of the models. The semi-detailed balance column refers to a property of the collision matrix which is a weak form of reversibility (see ref. 3 and Section 2 below). References in boldface contain results of numerical simulations. The values

Table I. Main Characteristics of Previously Introduced FCHC Models

Name	Collision rules	Optimization of v	Rest particles	Semi-detailed balance	$R_*^{\max}$ Boltzmann	Reference
FCHC-1	Algorithm	No	0	Yes	2.00	8, **9**
FCHC-2	Table	Approximate	0	Yes	6.44	10
FCHC-3	Table	Approximate	0	Yes	7.13	**7**, 10, **11**
FCHC-4	Table	Exact	0	Yes	7.57	10
FCHC-5	Table	Exact	3	Yes	10.71	10
FCHC-6	Table	Exact	0	No	17.2	12

of the Reynolds coefficient are computed under the *Boltzmann approximation.* Previous experience has shown that this approximation is remarkably good as long as semi-detailed balance is satisfied. As we shall see, it deteriorates markedly when semi-detailed balance is violated.

FCHC-1 is the *isometric model.* Collisions are defined by a *global rule*: the output state is computed from the input state according to a general algorithm. This model was used for the initial validation of the FCHC method. In all subsequent models, collisions are defined instead by an explicit table, giving the output state for every possible input state. One tries then to minimize the kinematic viscosity ν, in order to maximize the Reynolds coefficient. This was done by a heuristic, approximate method in models FCHC-2 and FCHC-3. These two models differ only by a minor change in the heuristics. Results of simulations were published only for FCHC-3, which has a slightly better Reynolds coefficient.

As the optimization algorithm was perfected, it became possible to compute the exact optimum in model FCHC-4 (and in all subsequent models). The latter represents the best which can be achieved within the bounds of the original definition of the FCHC lattice,[6] i.e., with a maximum of 24 moving particles, and assuming semi-detailed balance.

One way to increase the Reynolds coefficient, as shown by d'Humières and Lallemand,[5] is to add rest particles: more collisions are allowed, thereby giving more room for optimization. However, in three dimensions, the size of the collision table grows rapidly with the number of rest particles. For existing machines, the practical limit for that number is three (see Section 7). This was realized in model FCHC-5.

Semi-detailed balance implies universal properties, i.e., independence on the collision rules, for equilibrium distribution, and thus for the Galilean factor $g(d)$. This condition, together with the Boltzmann approximation, implies positivity of the viscosity.[13] This suggests that one should be able to obtain a lower, perhaps even negative, viscosity by dropping that condition. For the 24-velocity model (no rest particles), an optimal collision table is then easily derived: for each input state, one simply chooses the "best" output state. This gives model FCHC-6. The procedure indeed reduces the (Boltzmann-based) viscosity; it remains, however, positive.

The next idea is to combine the approaches of models FCHC-5 and FCHC-6, i.e., to incorporate simultaneously rest particles and violation of semi-detailed balance. An example is model FCHC-7, to be described in the present paper.

Finally, following an idea due to Somers and Rem,[14] one can note that the Galilean factor $g(d)$, which appears multiplicatively in the Reynolds coefficient, becomes a function of the collision rules when semi-

detailed balance is violated.[12] Therefore one can also try to maximize that factor. This leads to model FCHC-8, which also will be described in the present paper.

1.2. Outline

Definitions of the lattice gas models used are given in Section 2. The Boltzmann approximation is introduced in Section 3. This approximation is at present the only analytical tool allowing us to estimate theoretically the Galilean factor $g(d)$ and the kinematic viscosity ν, which are both functions of the collision rules, when the assumption of semi-detailed balance is violated. In Section 4 the Boltzmann approximation is used to construct explicit low-velocity equilibrium solutions. The Galilean factor, the viscosity, the speed of sound, and the Reynolds coefficient are obtained in Section 5 on transport coefficients. Optimization of the collision rules with respect to the (Boltzmann-based) transport coefficients is discussed in Section 6. We show that most of the questions asked can be reduced to a standard optimization problem, known as the *Hitchcock* or *transportation problem*. Results of this optimization problem are presented in Section 6.3; this is where we see negative viscosities appearing for the first time for FCHC models.

In Section 7 we explain in some detail how the models can be implemented in three-dimensional simulations; in particular, we show how to construct the collision (lookup) table. In Section 8 careful measurements of *true* (not Boltzmann-based) transport coefficients are presented for the new FCHC-7 and FCHC-8 models and for the previously introduced FCHC-3 model. Simulations of realistic flows (with boundaries, etc) are not within the scope of this paper (see, e.g., refs. 7–11).

Section 9.1 is a summary of the main results. In Section 9.2 we discuss the origin of the significant discrepancies observed between true and Boltzmann values when semi-detailed balance is violated and we suggest remedies. In the last Section 9.3, an interesting issue raised by Orszag and Yakhot[15] is revisited for models possessing high Reynolds coefficients.

Material presented in this paper is not always in the order in which the questions were investigated chronologically. For example, the simultaneous optimization of viscosity and Galilean factor (Section 6.4) was suggested to us by J. A. Somers and P. C. Rem after implementation of self-dual models had produced results which were somewhat disappointing (by reference to Boltzmann-based expectations).

Two-dimensional lattice gas models are not discussed in this paper, but we note that all the FCHC models may be used projected down from four to two rather than three dimensions. Unpublished results of one of us

(J.P.R.) have shown that this provides an efficient simulation tool on machines possessing a very large memory. However, alternative, possibly simpler two-dimensional algorithms with high Reynolds coefficients, based on non-strictly-local collision rules, have been proposed and appear promising.[16,17]

2. DEFINITIONS

We shall use in this paper variants of the early 24-bit FCHC models[3,6,7] with rest particles and modified collision rules. As usual, D denotes the dimension of space ($D=4$ for the FCHC lattice, its three-dimensional implementation included; see Section 7.3); the position of a node is defined by a set of signed integers $\mathbf{x}=(x_1,...,x_D)$. For the FCHC lattice, their sum is even. As usual, Greek letters α, β,... denote Cartesian coordinate indices, while Roman letters are used to distinguish different sorts of particles (by their velocities). Small Roman indices such as i refer to moving particles; capital Roman indices such as I refer to moving or rest particles, the latter being ascribed the index zero. Implicit summation on repeated Greek indices is assumed.

The nonzero velocities are $\mathbf{c}_i$, $i=1$ to b, with components $c_{i\alpha}$. All the FCHC models have $b=24$. Rest particles have velocity $\mathbf{c}_0=0$. For each velocity $\mathbf{c}_i\neq 0$ at most one particle is allowed (exclusion principle). The maximum allowed number of rest particles n_0 may be greater than one. All particles have the same mass. A composite index such as Ik refers to situations with k particles of velocity index I at a node; for example, P_{Ik} is the probability to have k particles of velocity index I. For $I>0$, when the index $k=1$ (its maximum value), it will often be omitted; for example, P_i denotes the probability of having one particle of velocity $\mathbf{c}_i$. Note that this quantity was denoted N_i in previous publications.

A state characterizing a given node is a collection of integers $s=(s_I)$ satisfying

$$0\leqslant s_0\leqslant n_0, \qquad s_i=0 \text{ or } 1, \quad i=1,...,b \tag{4}$$

s_I is the number of particles with velocity $\mathbf{c}_I$. The *dual* of a state $s=(s_I)$ is the state $\bar{s}=(\bar{s}_I)$ with $\bar{s}_i=1-s_i$ and $\bar{s}_0=n_0-s_0$. Note that for moving particles, this means interchanging particles and holes (i.e., absence of particle).

Input states (before collision) are denoted

$$s=(s_0, s_1,..., s_b) \tag{5}$$

Output states (after collision) are denoted

$$s'=(s'_0, s'_1,..., s'_b) \tag{6}$$

Note that the number of distinct states per node is $(n_0+1)\,2^b$. The number of moving particles in a state s at a node is

$$p_+ = \sum_{i=1}^{b} s_i \tag{7}$$

and the total number of particles is

$$p = \sum_{I=0}^{b} s_I = s_0 + p_+ \tag{8}$$

We now turn to the dynamical aspects of the lattice gas models. We take as unit of time the time required by one propagation step. The unit of length was implicitly defined by the specification of the FCHC lattice at the beginning of the present section (nodes have integer coordinates). The link length is $\sqrt{2}$ (distance from a node to its nearest neighbors). The speed of the moving particles is therefore $c=\sqrt{2}$. We take as unit of mass the mass of a particle.

The rules of the lattice gas automaton are defined in the usual way.[3] Particles with nonzero speed propagate to nearest neighbor and rest particles stay put. Collisions are controlled by transition probabilities

$$A(s \to s') \tag{9}$$

from input states s to output states s'. The set $A(s \to s')$ is called the collision matrix. Normalization of probability is assumed:

$$\sum_{s'} A(s \to s') = 1, \qquad \forall s \tag{10}$$

Semi-detailed balance,[3] which is defined like (10), but with summation over s, is *not* assumed. Lack of semi-detailed balance for deterministic models (i.e., such that there is a single output state to which a given input state has a nonvanishing transition probability) means that different input states can map to the same output state.

As usual, it is assumed that mass and momentum are conserved in individual collisions:

$$\begin{aligned} A(s \to s') \sum_I (s'_I - s_I) &= 0 \\ A(s \to s') \sum_I (s'_I - s_I)\,\mathbf{c}_I &= 0, \qquad \forall s, s' \end{aligned} \tag{11}$$

A model is said to be *self-dual* if

$$A(\tilde{s}, \tilde{s}') = A(s, s'), \qquad \forall s, s' \tag{12}$$

where $\bar{s}$ and $\bar{s}'$ are the duals of s and s'. Additional constraints on the collision matrix will result from the assumption of a prescribed basic equilibrium (Section 4.1). Finally, full invariance under the crystallographic group (G-invariance)[3,13] for the collision laws is assumed when working out the theory.

3. THE BOLTZMANN APPROXIMATION

As usual, the Boltzmann approximation consists in neglecting correlations between particles entering collisions. The physical idea underlying the Boltzmann approximation is that the propagation step following immediately the collision step suppresses most of the correlations which may have been generated in collisions. Use of the Boltzmann approximation may introduce errors in the description of both steady-state solutions with uniform hydrodynamic velocity (usually called "equilibria") and steady-state solutions with uniform shear. In the previously explored framework, with the condition of semi-detailed balance satisfied (models FCHC-1 to FCHC-5), the Boltzmann approximation was exact for equilibria (because their probability distribution is then completely factorized) and gave reasonably accurate predictions for the viscosity. With violations of semi-detailed balance the approximation may (and will actually) deteriorate. Our hope is that the Boltzmann approximation is still a useful guide in the fine tuning of the collision rules when trying to achieve the highest possible Reynolds coefficients.

Within the Boltzmann approximation, the statistics of the lattice are completely described by the set of probabilities

$$P_{Ik}(t, \mathbf{x}) = \Pr\{s_I(t, \mathbf{x}) = k\} \tag{13}$$

where $s(t, \mathbf{x})$ is the input state at discrete time t and discrete node $\mathbf{x}$. Normalization implies

$$\sum_k P_{Ik} = 1, \qquad \forall I \tag{14}$$

Note that for moving particles, the correspondence with the earlier notation N_i is

$$P_{i1} \equiv P_i = N_i, \qquad P_{i0} = 1 - N_i \tag{15}$$

The relevant hydrodynamic quantities can be defined in terms of these probabilities:

The mean density

$$\rho = \sum_{I,k} k P_{Ik} \tag{16}$$

The mean density of the moving particles

$$\rho_+ = \sum_i P_i \tag{17}$$

The mean mass flux

$$\mathbf{j} = \sum_i P_i \mathbf{c}_i \tag{18}$$

The mean velocity

$$\mathbf{u} = \frac{\mathbf{j}}{\rho} \tag{19}$$

The mean velocity of the moving particles

$$\mathbf{u}_+ = \frac{\mathbf{j}}{\rho_+} \tag{20}$$

Note that ρ is the density *per node*, not per unit volume; in order to obtain the density in the usual sense, one should multiply it by a factor equal to the number of nodes per unit D-dimensional volume (1/2 for FCHC). The same remark applies to ρ_+ and to $\mathbf{j}$.

The (lattice) Boltzmann equation takes the form

$$P_{Ik}(t+1, \mathbf{x}+\mathbf{c}_I) = \sum_s \sum_{s'} \delta(s'_I, k)\, A(s \to s') \prod_J P_{Js_J}(t, \mathbf{x}) \tag{21}$$

In the rhs, the Kronecker delta $\delta(s'_I, k)$ selects the output states having exactly k particles of velocity $\mathbf{c}_I$. In the lhs, the space-time shifts correspond to propagation. Because of (14) the above set of equations is redundant and we may restrict consideration to the set of $n_0 + b$ equations having $k > 0$. Using (10), we may rewrite the Boltzmann equation as

$$P_{Ik}(t+1, \mathbf{x}+\mathbf{c}_I) - P_{Ik}(t, \mathbf{x}) = \Delta_{Ik}(t, \mathbf{x}) \tag{22}$$

where

$$\Delta_{Ik} = \sum_s \sum_{s'} [\delta(s'_I, k) - \delta(s_I, k)]\, A(s \to s') \prod_J P_{Js_J} = 0 \tag{23}$$

is called the collision term.

4. EQUILIBRIUM SOLUTIONS

4.1. Basic Equilibrium (Zero Velocity)

Equilibrium solutions, independent of space and time, are obtained by setting the collision term to zero. An important role in the subsequent

analysis is played by *basic equilibrium* solutions. These are solutions with vanishing mean velocity which are consistent with the G-invariance. It follows that the probability of one (respectively, zero) particle with non-vanishing velocity P_{i1} (respectively, P_{i0}) is independent of i, and will be denoted by $d_{i1} = d$ (respectively, $d_{i0} = 1 - d$). For rest particles, P_{0k} will be denoted d_{0k}. Normalization implies

$$\sum_{k=0}^{n_0} d_{0k} = 1 \tag{24}$$

A basic equilibrium is therefore defined by $n_0 + 1$ independent quantities $\{d, (d_{0k}, k = 1,..., n_0)\}$. The Boltzmann equation for the basic equilibrium takes the form

$$d_{Ik} = \sum_s \sum_{s'} \delta(s'_I, k)\, P(s)\, A(s \to s'), \qquad \forall I, k \tag{25}$$

Here, $P(s)$, the probability of an input state in basic equilibrium, is given by

$$P(s) = \prod_J d_{Js_J} = d_{0s_0} d^{p_+} (1-d)^{b-p_+} \tag{26}$$

Equations (25) are redundant. For $I > 0$ and $k = 1$ (moving particles) they are all identical. Multiplying (25) by k and summing over I and k, we obtain an identically verified equation, expressing the conservation of mass. Therefore we can omit the equation for $I > 0$. We are left with the conditions

$$\sum_s \sum_{s'} \delta(s'_0, k)\, P(s)\, A(s \to s') = d_{0k}, \qquad \forall k > 0 \tag{27}$$

One possible approach, which was followed in ref. 12, is to assume nothing about the collision matrix apart from the conservation conditions (11). A practical problem with this approach is that the basic equilibrium is not known; it is given by the system of nonlinear equations (27), which cannot be solved explicitly, and which may have more than one solution. Therefore a different approach will be used here. We shall consider the probabilities d and d_{0k}, characterizing basic equilibria as given. Equations (27) represent then additional constraints which must be satisfied by the collision matrix A.

We stress that the equilibrium solutions derived here are obtained in a formal way, within the Boltzmann approximation and without reference at this point to their stability. We shall see in Section 6 that

negative viscosity instabilities are present in some of the models (still in the Boltzmann framework). Implementations demonstrating the actual existence of basic equilibria will be postponed to Section 8.

4.2. Equilibria with Uniform Mean Flow

As shown in ref. 12, in the absence of semi-detailed balance, equilibrium solutions lose the universality property with respect to the collision matrix.[3] Use of the Boltzmann approximation allows, however, explicit calculation of the equilibrium solutions for small hydrodynamic velocities, by perturbation around the basic equilibrium solution.[12] We are thus led to seek solutions of Eq. (22) in the form

$$P_i(\rho, \mathbf{u}) = d + \chi \mathbf{c}_{i\alpha} u_\alpha + \mu Q_{i\alpha\beta} u_\alpha u_\beta + \eta \delta_{\alpha\beta} u_\alpha u_\beta + O(\mathbf{u}^3) \tag{28}$$

$$P_{0k}(\rho, \mathbf{u}) = d_{0k} + \eta_{0k} \delta_{\alpha\beta} u_\alpha u_\beta + O(\mathbf{u}^3) \tag{29}$$

where d and the d_{0k} characterize a basic equilibrium and the tensor $Q_{i\alpha\beta} = c_{i\alpha} c_{i\beta} - (c^2/D)\, \delta_{\alpha\beta}$ is traceless. The relatively simple form of the coefficients is dictated by the G-invariance: invariant vectors $t_{i\alpha}$ must be proportional to $c_{i\alpha}$ and invariant tensors $t_{i\alpha\beta}$ must be a linear combination of $Q_{i\alpha\beta}$ and $\delta_{\alpha\beta}$ (see ref. 3).

The coefficient χ in (28) is obtained by identifying the mean velocity. This gives

$$\chi = \frac{\rho D}{bc^2} \tag{30}$$

For the $n_0 + 2$ remaining coefficients μ, η, and η_{0k} it is necessary to substitute (28) and (29) into the Boltzmann equation (22) and to require that the collision term Δ_{ik} given by (23) should vanish up to second order in the mean velocity. G-invariance implies that the collision term has an expansion similar to (28)–(29) without terms of order zero and one. This follows from the observation that the collision term has to be orthogonal to constants and to the $\mathbf{c}_i$'s (by mass and momentum conservation). Such properties can be used to simplify the evaluation of the coefficients μ, η, and η_{0k}. The details, quite similar to those already presented in ref. 12, will be omitted. Explicit expressions for the coefficients η and η_{0k} require the solution of a system of linear equations with n_0 unknowns which seemingly cannot be further simplified by the use of symmetries. In the sequel, we shall only need the coefficient μ, which has an explicit expression

$$\mu = \frac{d}{1-d} \left(\frac{\rho}{bd} \right)^2 \frac{D^2}{2c^4} \left(1 - 2d - \frac{\phi}{\psi} \right) \tag{31}$$

Here,

$$Nd(1-d)\,\phi = \sum_s \sum_{s'} P(s)\,A(s \to s')\,q_\alpha q_\beta (Y'_{\alpha\beta} - Y_{\alpha\beta}) \tag{32}$$

$$Nd(1-d)\,\psi = \sum_s \sum_{s'} P(s)\,A(s \to s')\,Y_{\alpha\beta}(Y'_{\alpha\beta} - Y_{\alpha\beta}) \tag{33}$$

$$N = \frac{bc^4(D-1)}{D} \tag{34}$$

(35)

where

$$q_\alpha = \sum_i s_i \mathbf{c}_{i\alpha} \tag{36}$$

and

$$Y_{\alpha\beta} = \sum_i s_i Q_{i\alpha\beta}, \qquad Y'_{\alpha\beta} = \sum_i s'_i Q_{i\alpha\beta} \tag{37}$$

are respectively the first- and second-order velocity moments of a state s (see refs. 12 and 13).

We note that the expression for μ obtained above is similar to the one obtained in the case without rest particles.[12] The only change is that the probability $P(s)$ of a state in basic equilibrium is now $\prod_J d_{Js_J}$ instead of $d^p(1-d)^{b-p}$.

Finally, we observe that μ vanishes when $d = 1/2$ for self-dual models. Indeed, under the duality transformations ($_i \to 1 - s_i$), the velocity $\mathbf{u}$ is reversed, the probabilities P_i are changed into $1 - P_i$, and the density d into $1 - d$. Hence, in the expansion (28), the coefficients of terms quadratic in $\mathbf{u}$ must vanish. Alternatively, the vanishing of μ can be checked from its expression (31): under duality the first- and second-order moments q_α and $Y_{\alpha\beta}$ change sign; this implies the vanishing of ϕ, given by (32), for self-dual models and self-dual densities (i.e., $d = 1/2$).

5. TRANSPORT COEFFICIENTS

5.1. The Galilean Factor $g(d)$

It was shown in ref. 3 that lattice gas models lead to the incompressible Navier–Stokes equations in suitable large-scale and low-velocity limits. This was done in detail for models with no rest particles and satisfying the condition of semi-detailed balance. The generalization to models

with rest particles and without semi-detailed balance involves only minor technical modifications. As usual, the Navier–Stokes equations are obtained with a nonlinear term modified by a Galilean factor $g(d)$ which is constant in the incompressible (low-Mach-number) limit and which can be removed by rescaling the time variable.

Proceeding exactly as in ref. 3, we can relate $g(d)$ to the coefficient μ of quadratic terms in the equilibrium distribution (28):

$$g(d) = \frac{2bc^4}{\rho D(D+2)}\,\mu \tag{38}$$

Using (31) and $\rho_+ = bd$, we obtain

$$g(d) = \left(\frac{\rho}{\rho_+}\right)\frac{D}{D+2}\,\frac{1}{1-d}\left(1 - 2d - \frac{\phi}{\psi}\right) \tag{39}$$

ϕ and ψ being given by (32) and (33). Note that, in the case when semi-detailed balance holds, ϕ is zero and we recover the result of d'Humières and Lallemand.[5] Without semi-detailed balance, the Galilean factor loses its universality and becomes dependent on the details of the collision matrix. Note, finally, that when self-duality holds, and irrespective of the assumption of semi-detailed balance, $g(d)$ vanishes for $d = 1/2$, a consequence of the vanishing of μ (see end of Section 4.2).

5.2. The Speed of Sound

The computations of Section 7.1 in ref. 3 can be extended in a straightforward manner to the present case and give the following expression for the speed of sound:

$$c_s = \frac{c}{\sqrt{D}}\left[1 + \frac{\sum_k k^2 d_{0k} - (\sum_k k d_{0k})^2}{bd(1-d)}\right]^{-1/2} \tag{40}$$

Although the collision matrix does not appear in this expression, the derivation assumes that the rest particles and the moving particles are coupled by the collisions, so that local equilibrium is maintained between them. (It would be invalid in the special case where the number of rest particles is preserved in collisions.) Incidentally, it can be shown that the quantity inside brackets is always larger than 1: the presence of rest particles slows down sound propagation.

We will also need the ratio ρ/ρ_+. From (16) and (17) we find for the basic equilibrium

$$\frac{\rho}{\rho_+} = 1 + \frac{\sum_k k d_{0k}}{bd} \tag{41}$$

5.3. The Kinematic Viscosity

The kinematic viscosity can be obtained by considering steady-state solutions of the Boltzmann equations (22) having uniform shear. This is a straightforward extension of the analysis performed in ref. 13. We list only the main points, omitting details. Composite equation numbers such as (2.27) will refer to ref. 13 in the present section. The notation v_i (and its generalization v_{Ik}) is also taken from ref. 13; it denotes changes in the basic equilibrium probabilities resulting from the application of a weak shear. This notation must be distinguished from the kinematic viscosity v.

We note first that semi-detailed balance is not actually required for the derivation of the viscosity in ref. 13. The first term in (2.27) vanishes in any case, since $v_j = 0$ corresponds to the basic equilibrium. Thus, even without semi-detailed balance, (3.38) and (4.5) hold, and it is only necessary to extend the treatment so as to include rest particles.

We assume that the mean velocity is a uniform weak shear flow:

$$u_\alpha = \sum_\beta T_{\alpha\beta} x_\beta \tag{42}$$

and we compute first-order expansions of the P_{Ik}:

$$P_{Ik}(\mathbf{x}) = d_{Ik} + v_{Ik}(\mathbf{x}) \tag{43}$$

with

$$v_{Ik}(\mathbf{x}) \ll 1 \tag{44}$$

Symmetry considerations can be used to show that the probabilities for the rest particles are unperturbed to that order:

$$v_{0k} = 0, \qquad \forall k \tag{45}$$

The computation is then essentially the same as in ref. 13, with the quantity $d^p(1-d)^{n-p}$ replaced by $P(s)$. The kinetic viscosity is given by

$$v = \frac{c^2}{D+2}\left(\lambda - \frac{1}{2}\right) \tag{46}$$

where the quantity λ (which can be interpreted as a mean free path) is now given by

$$\frac{1}{\lambda} = \frac{1}{D-1} \sum_s \sum_{s'} (s_i - s_i')\, P(s)\, A(s \to s') \times \frac{1}{d(1-d)} \sum_j s_j (D \cos^2 \theta_{ij} - 1) \tag{47}$$

(Note that the rightmost term 1 cannot be delected, as in ref. 13, in the present case.) θ_{ij} is the angle between velocities, and i has an arbitrary value. A rearrangement similar to (4.1)–(4.9) gives

$$\frac{1}{\lambda}=\frac{D}{(D-1)\,bc^4}\sum_s\sum_{s'}P(s)\,A(s\to s')\frac{1}{d(1-d)}\,Y_{\alpha\beta}(Y_{\alpha\beta}-Y'_{\alpha\beta}) \tag{48}$$

Comparing with (33), we find that

$$\frac{1}{\lambda}=-\psi \tag{49}$$

5.4. The Reynolds Coefficient R_*

We are now in a position to evaluate the "Reynolds coefficient" which characterizes the ability of a given model to achieve high Reynolds numbers.[3,7] When the scale l_0 and the characteristic velocity u_0 of a flow are expressed in standard lattice units (Section 2), the Reynolds number R is given by[3]

$$R=l_0u_0\frac{g(d)}{\nu} \tag{50}$$

where $g(d)$ and ν are the Galilean factor and the kinematic viscosity.

For models without rest particles, the Reynolds coefficient was defined as $R_*=c_sg(d)/\nu$. It incorporates the speed of sound c_s because the smallness of the Mach number $M=u_0/c_s$ is needed for the validity of the incompressible approximation. The Reynolds number is then given by[3]

$$R=Ml_0R_* \tag{51}$$

For models with rest particles, given the way we have defined the hydrodynamic velocity **u**, namely mass flux **j** divided by total density ρ (moving and rest particles), we are led to propose a modification of the definition of the Mach number and of the Reynolds coefficient.

We redefine the Mach number as

$$M=\frac{u_{0+}}{c_s} \tag{52}$$

where u_{0+} is the typical value for the velocity $\mathbf{u}_+$, based only on *moving* particles (20). It is easily checked that the modified Mach number is a better measure of the validity of the incompressible approximation. With the

previous definition, arbitrary increase in the number of rest particles would lead to arbitrary decrease of the Mach number, without actually improving incompressibility. The appropriate new definition of the Reynolds coefficient consistent with Eq. (51) is

$$R_* = \frac{u_0}{u_{0+}} \frac{c_s g}{\nu} = \frac{\rho_+}{\rho} \frac{c_s g}{\nu} \tag{53}$$

Note that the ρ_+/ρ factor cancels the inverse factor in (39).

6. OPTIMIZATION OF THE COLLISION RULES

6.1. Minimization of the Viscosity

In order to maximize R_* given by (53), we try to minimize the kinematic viscosity ν. In view of (46) and (49), this is equivalent to minimizing ψ given by (33). The adjustable parameters are: the number of rest particles n_0; the values d and d_{0k} which characterize the basic equilibrium; the collision probabilities $A(s \to s')$, subject to the conditions (10), (11), and (27). Our strategy will be to consider n_0, d, and the d_{0k} as given and to compute the optimal values of the $A(s \to s')$.

The constant factors in (33) can be ignored. We can also ignore the term $Y_{\alpha\beta} Y_{\alpha\beta}$, which gives on summation over s and s' a value independent of the collision probabilities $A(s \to s')$. Our problem is thus to choose the $A(s \to s')$ so as to minimize the quantity

$$\sum_s \sum_{s'} P(s)\, A(s \to s')\, Y_{\alpha\beta} Y'_{\alpha\beta} \tag{54}$$

subject to the constraints (10), (11), and (27). The self-duality constraint (12) will also be assumed except in Section 6.4.

We define a *family* $f(p, \mathbf{q})$ as the set of all states which have a given number of particles p and a given momentum $\mathbf{q}$. (This was called a *packet* in ref. 10.) The relations (11) mean that $A(s \to s') = 0$ when s and s' belong to different families. Therefore we only have to consider the values of $A(s \to s')$ for s and s' belonging to the same family.

For a given input state s and a given number k, consider the subset $\mathcal{S}(s, k)$ of all output states s' such that (i) s' is in the same family as s and (ii) the number of output rest particles is $s'_0 = k$. Define

$$A(s, k) = \sum_{s' \in \mathcal{S}(s,k)} A(s \to s') \tag{55}$$

Note that $A(s, k)$ is, for a given input state s, the probability of obtaining k output rest particles. The constraints (10) and (27) can be written

$$\sum_k A(s, k) = 1, \qquad \forall s \tag{56}$$

$$\sum_s P(s)\, A(s, k) = d_{0k}, \qquad \forall k \tag{57}$$

They involve only the quantities $A(s, k)$. Therefore the values of the quantities $A(s \to s')$ can be freely redistributed inside a set $\mathscr{S}$: the conditions remain satisfied. Clearly, then, the optimal solution will use only the collision (or collisions) for which the quantity $Y_{\alpha\beta} Y'_{\alpha\beta}$ is minimal. We call $\mathscr{Y}(s, k)$ this minimal value of $Y_{\alpha\beta} Y'_{\alpha\beta}$ on the set $\mathscr{S}(s, k)$. [A preliminary task will consist in finding $\mathscr{Y}(s, k)$ and the associated output states for all s and k.] The quantity to be minimized is then

$$\sum_s \sum_k P(s)\, A(s, k)\, \mathscr{Y}(s, k) \tag{58}$$

This optimization problem is not in a standard form because of the presence of the factor $P(s)$ in (57). This can be remedied by introducing the joint probability of having an input state s and k output rest particles:

$$B(s, k) = P(s)\, A(s, k) \tag{59}$$

The constraints (56) and (57) become

$$\sum_k B(s, k) = P(s), \qquad \forall s \tag{60}$$

$$\sum_s B(s, k) = d_{0k}, \qquad \forall k \tag{61}$$

and the quantity to be minimized is

$$\sum_s \sum_k B(s, k)\, \mathscr{Y}(s, k) \tag{62}$$

This has the form of a classical *Hitchcock problem*, or *transportation problem*: find a matrix B for which the sums of the elements along rows and columns have prescribed values, and such that a given linear combination of the elements is minimal. This problem could in principle be solved by known techniques. However, it differs in a number of respects from the problems encountered in the case of semi-detailed balance[10]:

1. The problem cannot be separated into independent problems for the families, because the sum (61) runs across families.

2. The right-hand sides of (60) are density-dependent [through $P(s)$], so that the optimization problem must be solved separately for each value of the density d.
3. The weights of the rows and columns, given by the right-hand sides of (60) and (61), are not integers. One must then contend with round-off errors.

All this makes the problem harder to solve. In addition, the solution of the problem as stated so far consists generally of noninteger values for the quantities $A(s \to s')$; in other words, the collision algorithm is nondeterministic. This would mean a larger collision lookup table (several output states must be stored, together with their probabilities) and a longer computation time of the collisions (the output state must be chosen according to a table of probabilities).

6.2. The Method of *f*-Equilibria

The difficulties above can be avoided at the cost of introducing additional constraints. First, we shall demand that, in the basic equilibrium, the probability of having k rest particles is preserved not only globally, but also *separately inside each family*. Specifically, representing a family by f, we replace (27) by

$$\sum_{s \in f} \sum_{s' \in f} \delta(s'_0, k)\, P(s)\, A(s \to s') = \sum_{s \in f} \delta(s_0, k)\, P(s), \qquad \forall f, k \tag{63}$$

This will be called an f-equilibrium. Note that by summing over f we recover (27). Thus, (63) represents indeed a set of more detailed constraints. These constraints are comparatively mild, however: we still have much more freedom than in the case of semi-detailed balance.

We can then consider separately a given family f. Equation (10), specialized to f, becomes

$$\sum_{s' \in f} A(s \to s') = 1, \qquad \forall s \in f \tag{64}$$

and the quantity (54) to be minimized can be decomposed into a sum in which individual terms involve only one family and have the form

$$\sum_{s \in f} \sum_{s' \in f} P(s)\, A(s \to s')\, Y_{\alpha\beta}\, Y'_{\alpha\beta} \tag{65}$$

This takes care of the first difficulty. Next, we shall imagine that there exists some hidden additional information which leads to a subdivision of

each state s into a number of *microstates* σ.[10] This number will be called the *multiplicity* of the state s and is represented by $\mathscr{M}(s)$. All microstates corresponding to a given state s are equally probable; therefore the probability of an input microstate σ is

$$P(\sigma) = P(s)/\mathscr{M}(s) \tag{66}$$

The collision rules are now defined by a matrix of elements $\mathscr{A}(\sigma \to \sigma')$, giving the probability that an output microstate σ' will be produced for an input microstate σ. Equations (63)–(65) are still applicable, with s, s', and A replaced by σ, σ', and $\mathscr{A}$: the constraints become

$$\sum_{\sigma' \in f} \mathscr{A}(\sigma \to \sigma') = 1, \qquad \forall \sigma \in f \tag{67}$$

$$\sum_{\sigma \in f} \sum_{\sigma' \in f} \delta(s_0', k)\, P(\sigma)\, \mathscr{A}(\sigma \to \sigma') = \sum_{\sigma \in f} \delta(s_0, k)\, P(\sigma), \qquad \forall k \tag{68}$$

and the quantity to be minimized becomes

$$\sum_{\sigma \in f} \sum_{\sigma' \in f} P(\sigma)\, \mathscr{A}(\sigma \to \sigma')\, Y_{\alpha\beta}\, Y'_{\alpha\beta} \tag{69}$$

In (68) it is understood that s_0 and s_0' are the numbers of rest particles in the microstates σ and σ'.

Now we assume that the multiplicities are chosen in such a way that *all microstates of a family have the same probability*. From (26) and (66), we find that this will be the case if the multiplicities have the form

$$\mathscr{M}(s) \propto d_{0s_0} d^{p+} (1-d)^{b-p+} \tag{70}$$

Multiplying and dividing by $d^{s_0}(1-d)^{n_0 - s_0}$, and noting that the total number p of particles given by (8) is constant in a family, we can write this in the form

$$\mathscr{M}(s) \propto \frac{d_{0s_0}}{d^{s_0}(1-d)^{n_0 - s_0}} \tag{71}$$

We see that the multiplicity of a state s is a function of its number s_0 of rest particles only. Accordingly, we write it from now on in the form $\mathscr{M}_{s_0}$. The multiplicities must be integers; nevertheless, given a set of d_{0k}, Eq. (71) can in principle be satisfied with an arbitrarily small error by taking the multiplicities large enough. Conversely, given a set of multiplicities, the d_{0s_0} can be computed from (71). [The proportionality constant is obtained from the normalization (24).] The multiplicities $\mathscr{M}_k$ can thus be viewed simply as another way of defining the quantities d_{0k}.

Now $P(\sigma)$ is a constant inside a family f. Therefore it can be taken out of the summations and then eliminated in (68) and (69). We proceed as before: for a given input microstate σ and a given number k, we consider the subset $\mathscr{S}(\sigma, k)$ of all output microstates σ' obtainable from σ and having k rest particles. We define

$$\mathscr{A}(\sigma, k) = \sum_{\sigma' \in \mathscr{S}(\sigma,k)} \mathscr{A}(\sigma \to \sigma') \tag{72}$$

The constraints (67) and (68) can be written

$$\sum_{k} \mathscr{A}(\sigma, k) = 1, \qquad \forall \sigma \in f \tag{73}$$

$$\sum_{\sigma \in f} \mathscr{A}(\sigma, k) = \sum_{\sigma \in f} \delta(s_0, k), \qquad \forall k \tag{74}$$

They involve only the quantities $\mathscr{A}(\sigma, k)$. Again, the optimal solution will use only the collision (or collisions) for which the quantity $Y_{\alpha\beta} Y'_{\alpha\beta}$ is minimal. The minimum is the same quantity $\mathscr{Y}(s, k)$ as before, since $Y_{\alpha\beta}$ and $Y'_{\alpha\beta}$ are functions only of the state s. The quantity to be minimized is then

$$\sum_{\sigma \in f} \sum_{k} \mathscr{A}(\sigma, k)\, \mathscr{Y}(s, k) \tag{75}$$

Equations (73)–(75) represent again a Hitchcock problem. But now the parameter d has been completely eliminated. Thus, the optimization problem has to be solved only once, and the results can then be used for all values of d. We note also that the right-hand sides of the constraints (73) and (74) are now integers. As a result, the optimization problem can be solved exactly, with existing algorithms. Another interesting consequence is that a general theorem[18] states that in such a case, there exists an optimal solution in which all $\mathscr{A}(\sigma, k)$ are integers. Since the row sum must be 1 by (73), in every row one coefficient equals 1 and all the others vanish. In other words: a deterministic algorithm can be built, representable by a lookup table operating on the microstates.

In the particular case where the multiplicities are symmetrical, i.e.,

$$\mathscr{M}_{n_0 - k} = \mathscr{M}_k, \qquad \forall k \tag{76}$$

the optimization problem defined by (73)–(75) is invariant under duality. In that case, it is therefore sufficient to solve the problem for one-half of the families only, namely those for which the number of particles is $p \leqslant (n_0 + b)/2$, and to use duality to obtain the other half of the collision lookup table. This produces a self-dual model (Section 2). Note that the

condition (76) can be translated with the help of (71) into an equivalent condition for the d_{0k}:

$$\frac{d_{0,n_0-k}}{d_{0k}} = \left(\frac{d}{1-d}\right)^{n_0-2k} \tag{77}$$

A more special case is the *indistinguishable case*[10]:

$$\mathscr{M}_k = 1, \qquad \forall k \tag{78}$$

Microstates and states then become identical. This is the case which will be used in the implementations (see Section 7).

As in the case of semi-detailed balance,[10] the computation of the optimal solution can be considerably accelerated by taking as elementary objects the *species* instead of the states; a species is a subset of a family consisting of all states which can be changed into each other by isometries preserving the FCHC lattice.

6.3. Results

Figure 1 shows a closeup of the kinematic viscosity ν obtained by the above method in the vicinity of $d = 0.5$ (where it has a minimum), in the indistinguishable case. The solid lines correspond, respectively, from top to bottom, to $n_0 = 0$, 1, 2, 3, 7, 15, 31 rest particles. Table II lists the minimal values of ν.

It can be seen that the Boltzmann viscosity is negative over an interval of d values when n_0 is 2 or more. The figure also suggests that the minimum negative viscosity may have a finite limit for $n_0 \to \infty$. Since the viscosity depends continuously on d, there exists for each $n_0 \geqslant 2$ a critical density $0 < d_c < 1/2$ at which the viscosity vanishes.

For comparison, the dashed lines represent the Boltzmann viscosity in the case of semi-detailed balance,[10] again in the indistinguishable case, for 0, 1, 2, and 3 rest particles. The case $n_0 = 3$ is model FCHC-5. We recall that when semi-detailed balance is satisfied, the viscosity must remain positive[13] and an H-theorem holds (ref. 3, Appendix F).

As soon as the kinematic viscosity becomes negative, the basic equilibrium solutions described in Section 4.1, which are spatially uniform, lose stability. Presumably, new equilibria with nontrivial spatial structure will then emerge. This question will not be pursued here.

6.4. Simultaneous Optimization of ν and g

With a Boltzmann-based viscosity which can be tuned arbitrarily close to zero, as exhibited in the previous section, one can in principle build

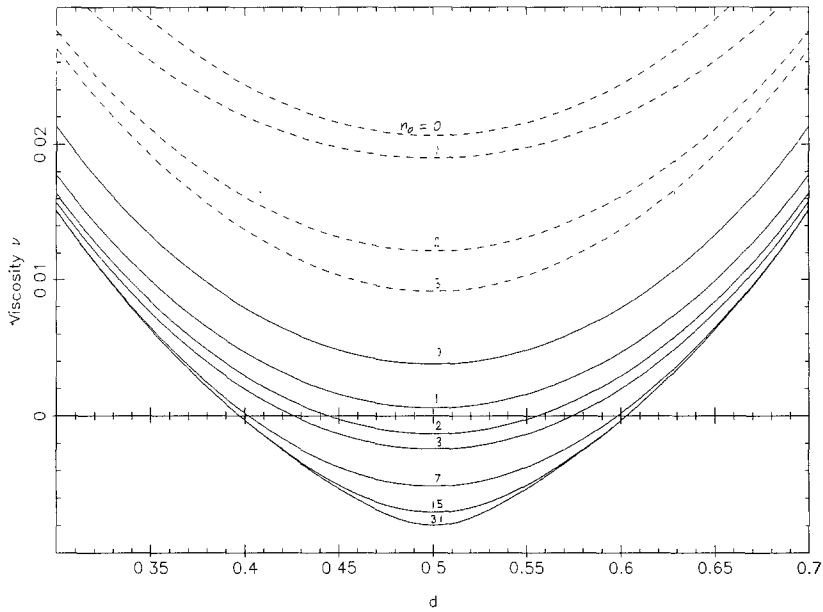

Fig. 1. Boltzmann-based kinematic viscosity ν as a function of d, in the indistinguishable case. The solid lines represent the computations of the present paper (no semi-detailed balance) with, from top to bottom, $n_0 = 0, 1, 2, 3, 7, 15, 31$ rest particles. For comparison, the dashed lines represent the viscosity in the case of semi-detailed balance,[10] again in the indistinguishable case, for 0, 1, 2, and 3 rest particles.

models with arbitrary large values of the Reynolds coefficient $R_*^{\max}$. Unfortunately, the true viscosity, measured in the three-dimensional simulations, will turn out to be noticeably larger than the Boltzmann viscosity, and definitely to remain positive (see Section 8, which the reader may want to read first). We therefore looked for other ways to improve the true $R_*^{\max}$,

Table II. Minimal Values of ν

n_0	$\nu(0.5)$
0	0.0038
1	0.0006
2	−0.0013
3	−0.0024
7	−0.0051
15	−0.0070
31	−0.0080

still using Boltzmann results as a guide, but with proper care. We now use an idea of Somers and Rem.[14] Equation (53) shows that the Reynolds coefficient depends not only on the viscosity ν, but also on various other factors. The factors ρ_+/ρ and c_s depend only on the densities d and d_{0k}, which are considered as given; therefore these factors can be left out of consideration. As already stressed in Section 5.1, without semi-detailed balance the Galilean factor $g(d)$ depends on the collision rules and not only on the densities d and d_{0k}.

In principle, one should then choose the collision matrix $A(s \to s')$ so as to maximize the ratio g/ν. Using (53), (39), and (46), we find that R_* can be expressed in terms of ϕ and ψ as

$$R_* = \frac{2Dc_s}{c^2(1-d)} \frac{\phi - (1-2d)\psi}{\psi + 2} \tag{79}$$

This is a nonlinear function of the entries $A(s \to s')$ of the collision matrix, and therefore the usual optimization algorithms cannot be applied. Anyway, we already know that R_* given by the Boltzmann expression (79) can take arbitrarily large values, since the Boltzmann viscosity can be tuned arbitrarily close to zero. Influenced by our knowledge that the true viscosity (not Boltzmann-based) stays positive (see Section 8.1), we shall adopt the following strategy. We want to simultaneously minimize ψ and maximize ϕ. Therefore we consider a linear combination

$$a_1\psi - a_2\phi \tag{80}$$

where a_1 and a_2 are given nonnegative coefficients, and we determine the $A(s \to s')$ which minimizes that combination. This is again a linear optimization problem, which can be solved exactly with existing algorithms. We adjust then the value of the ratio $a_1 : a_2$ so as to obtain the highest possible value of $R_*^{\max}$.

We remark that a ratio $a_1 : a_2 = 1:0$ corresponds to optimizing only the viscosity, i.e., to the model of the previous section. A high ratio like $a_1 : a_2 = 1000:1$ corresponds to optimizing the viscosity first, and then optimizing g. There may indeed be some further room for g optimization if multiple choices of the ν-optimal collision rules are permitted, a usual situation.[10] Experience shows that this already produces a substantial improvement. Indeed, Somers and Rem[14] were led heuristically to maximize a quantity [which they denote $F(s')$] which is easily shown to be essentially equivalent to our quantity ϕ. For an FCHC model without rest particles they obtained a Boltzmann-based $R_*^{\max}$ of about 40, to be compared with 17 for our model FCHC-6.

At the other extreme, a ratio $a_1 : a_2 = 0:1$ would correspond to

optimizing g only; and a ratio $a_1 : a_2 = 1 : 1000$ would correspond to optimizing g first, and then ν when there are multiple choices. This case was also considered in ref. 14 for the FCHC model without rest particles.

Our experimentation indicated that the best ratio is in the vicinity of $a_1 : a_2 = 5 : 1$. Of course, the Boltzmann value of $R_*^{\max}$ is of limited use as a guide for optimizing the true R_* and we were also limited by the fact that it is not practical to build and implement in full simulations models stemming from a large number of choices for the value of $a_1 : a_2$. The above ratio was therefore determined by a somewhat empirical mixture of these two sources of information. Thus, further improvements of the resulting model cannot be ruled out.

Another important remark for the optimization, also due to Somers and Rem,[14] is that in order to maximize $g(d)$, it is much better to abandon self-duality. The reason is that in the case of self-duality, g vanishes for $d = 1/2$ (Section 5.1). As a consequence, g is small in the vicinity of $d = 1/2$, which is the region where maximal values of R_* usually occur. If, on the other hand, self-duality is violated, much larger values of g can be obtained.[15] Note also that the expression (80) is not invariant under duality when $a_2 \neq 0$: ψ is invariant, but ϕ changes sign. Self-duality was assumed in all our previous models, but purely for reasons of convenience: only one-half of the collision lookup table has to be computed. Fortunately, there is no reason of principle why duality should be requested, and therefore we dispense with it in the present model.

The generalization of the optimization procedure described in Section 6.1 is straightforward. In (32) and (33), we can ignore the terms which depend only on the input state, because on summation over s and s' they produce a value which is independent of the collision rules. Thus, minimizing (80) is equivalent to minimizing

$$\sum_s \sum_{s'} P(s)\, A(s \to s')(a_1 Y_{\alpha\beta} - a_2 q_\alpha q_\beta)\, Y'_{\alpha\beta} \tag{81}$$

Therefore all we have to do is to replace everywhere the quantity $Y_{\alpha\beta} Y'_{\alpha\beta}$ by $(a_1 Y_{\alpha\beta} - a_2 q_\alpha q_\beta)\, Y'_{\alpha\beta}$.

Boltzmann values for this case will be given in Section 8, where they will be compared to true values.

7. IMPLEMENTING THE MODELS

In previous sections we have used the Boltzmann approximation and optimization techniques as a guide for discovering models with high Reynolds coefficients. In order to find the true values of the transport coef-

ficients for these models, it is necessary to perform appropriate simulations. They will be presented in Section 8. In the present section, we explain how to carry out efficient computer implementations of the models using a lookup table strategy. As noted in Section 6.2, all our optimal models can be implemented deterministically, i.e., by lookup table.

7.1. Models FCHC-7 and FCHC-8

A convenient machine for implementing the FCHC models is the CRAY-2, which possesses 256 Mwords of 64 bits in its central memory. Implementation of model FCHC-3 on a CRAY-2 was briefly presented in ref. 7. Being a 24-bit model, it used a collision lookup table of 2^{24} words of 24 bits. This allows further substantial increases in the size of the collision lookup table to accommodate rest particles. Practical considerations related to machine availability led us not to exceed about 64 millon entries for the collision lookup table.

In order to construct the collision lookup table, we must specify the number n_0 of rest particles and the multiplicities $\mathscr{M}_k$ introduced in Section 6.1, which are in principle arbitrary integers. The total number of entries equals the number of microstates, i.e., $2^{24} \times \sum_{k=0}^{n_0} \mathscr{M}_k$. In practice this means that the multiplicities should be small integers. We selected the simplest indistinguishable case with all $\mathscr{M}_k$ equal to one. Indeed, experimentation with various multiplicity values in the case of semi-detailed balance[10] showed the indistinguishable case to be only marginally inferior to the best combination. Furthermore, the indistinguishable case permits the construction of exactly self-dual models (when desired). With this choice, the total number of entries of the collision lookup table is then $2^{24}(n_0+1)$.

We thus decided to have a maximum of $n_0 = 3$ rest particles, coded on two additional bits. In the present formalism, these bits are to be considered as representing an integer between 0 and 3, giving the number of rest particles in the state. In an alternative formalism, not implemented here, one could consider that these two bits are separate, and describe the presence or absence of one rest particle and of a "molecule" of two rest particles, respectively, as in the 8-bit, two-dimensional model of d'Humières and Lallemand.[5]

We are now in a position to completely specify models FCHC-7 and FCHC-8. Both models have a maximum number of $n_0 = 3$ indistinguishable rest particles. For model FCHC-7 the collision lookup table is computed according to the prescription of Section 6.1, that is, with optimization performed only on the viscosity. Self-duality is assumed, but no semi-detailed balance. For model FCHC-8 the collision lookup table is computed accor-

ding to the prescription of Section 6.4, that is, with optimization performed jointly on the viscosity and the Galilean factor. Neither semi-detailed balance nor self-duality is assumed.

We now list some useful relations, valid for both models, obtained by specializing previously established relations to the case of three indistinguishable rest particles.

The probability of having $k (0 \leqslant k \leqslant 3)$ rest particles at a node is, in the basic equilibrium,

$$d_{0k} = \frac{d^k (1-d)^{3-k}}{d^2 + (1-d)^2} \tag{82}$$

The speed of sound, computed from (40), is

$$c_s = \frac{1}{\sqrt{2}} \left[1 + \frac{1 + 4d^2(1-d)^2}{24[d^2 + (1-d)^2]^2} \right]^{-1/2} \tag{83}$$

The fraction of particles which are moving is

$$\frac{\rho_+}{\rho} = \left[1 + \frac{1 + 2d^2}{24[d^2 + (1-d)^2]} \right]^{-1} \tag{84}$$

7.2. Construction of the Collision Lookup Tables

The symmetries of the lattice can be used to reduce the work of computing optimal collision lookup tables. Details are given in ref. 10. Two families which differ only by an isometry (this means that they have the same number of particles p and that their momenta can be deduced from each other by an isometry) present essentially the same optimization problem, which needs to be solved only once. An additional advantage of the reduced table is that it fits on a single tape and is easily transported. Therefore the first step consists in computing a *reduced table*, in which only families with a *normalized momentum*[8] appear. If the model is self-dual, it is also sufficient to consider only the families for which the number of particles p does not exceed one-half of the maximum number $n_0 + b$. The computations of reduced tables were made on a SUN 3/60. The formulas of Section 6 were used, with a specially devised optimizing algorithm which takes advantage of the peculiarities of the problem.[10] The optimization problem is degenerate: more than one output state can usually be assigned to a given input state without affecting the viscosity. When multiple choices are possible, it is advantagous to make a random choice, which is performed while generating the table, so that the randomness becomes frozen.

These random choices are found to make the collision matrix "effectively isotropic" in the sense that the residual anisotropies of the viscosity tensor are less than the level of Monte Carlo noise in the output (see ref. 7).

On a CRAY-2, which has a large memory and hard-wired indirect addressing, it is best to use a full collision lookup table, in which all possible input states appear explicitly as entries. The "computation" of a collision is then reduced to a simple table lookup. A second preparatory step consists therefore in computing an *expanded table*, using isometries and duality (when applicable) to obtain the postcollision (output) state for any precollision (input) state. We explain now the details of this process, starting with the model FCHC-3 (described without details in ref. 7) and then indicate the changes needed for the two new models introduced in the present paper (FCHC-7 and FCHC-8).

7.2.1. Expanded Collision Lookup Table for Model FCHC-3

There are no rest particles. The full collision table has thus 2^{24} entries, each one requiring 24 bits for storage. For efficiency reasons, each entry is actually stored in a 64-bit CRAY word. This wastes memory, but saves execution time. The model is self-dual, that is, the collision table is invariant under particle–hole exchanges. Accordingly, the reduced table contains only input states with 0–12 particles.

To build the expanded table, we perform successively the following operations for each input state:

1. If the number of particles in the input state s is larger than 12, define s_* to be the dual $\bar{s}$ of s (interchange 0's and 1's); otherwise, take $s_* = s$.
2. Find a lattice-preserving isometry T that transforms the state s_* into a *normalized* input state s_{**} (a state with a normalized momentum; see ref. 8).
3. Use the reduced table to obtain the normalized output state s'_{**} corresponding to s_{**}.
4. Apply the inverse isometry T^{-1} to s'_{**} to obtain the state s'_*.
5. If duality was not used in the first step, the output state is $s' = s'_*$; otherwise, it is the dual $s' = \bar{s}'_*$.

Note that the isometry transforming s_* into a normalized state s_{**} is usually not unique. We shall come back to this in Section 7.2.2.

7.2.2. Expanded Collision Lookup Tables for Models FCHC-7 and FCHC-8

Models FCHC-7 and FCHC-8 have up to three indistinguishable rest particles per lattice node. The state of one node requires thus 26 bits for storage (24 for moving particles plus two extra bits to encode the rest particles). The full collision lookup table has 2^{26} entries, each one stored on 26 bits. At execution time, one entry is stored in one 64-bit CRAY word for efficiency reasons. On the mass storage device, however, two entries are stored in one word to reduce the transfer time between the mass storage and the mainframe at the beginning of each run.

The procedure for the construction of the expanded collision lookup tables from their reduced versions is similar to that used for model FCHC-3, with the following changes.

For model FCHC-8, duality is not used because the model is not self-dual. For both models, a further randomization, which takes advantage of the nonuniqueness of the isometry transforming s_* into a normalized state s_{**}, has been found necessary to eliminate residual anisotropies of the collision lookup tables.[5] Specifically, after the step leading to s_{**}, a lattice-preserving isometry R, randomly chosen among those which also preserve the momentum of s_{**}, is applied to the normalized state s_{**}, producing another normalized state s_{***}. The reduced table gives the corresponding output state s'_{***} (just as for model FCHC-3); this leads to s'_{**} after application of R^{-1}. The end of the procedure is the same as for FCHC-3.

7.3. The Three-Dimensional Implementations of FCHC Models

As they are defined, the FCHC models are four-dimensional. They may nevertheless be used in a *pseudo-4D* version for three-dimensional simulations. This was suggested in ref. 6 and verified in the first implementation.[9] A somewhat loose description of the pseudo-4D model in previous publications leads us to give now a more formal definition. Consider a four-dimensional FCHC lattice of infinite extent in all dimensions. It is the set of quadruplets of signed integers (x_1, x_2, x_3, x_4) such that the sum $x_1 + x_2 + x_3 + x_4$ is even. The geometrical lattice is periodic of period *two* in, say, the x_4 direction. If the lattice gas initial condition at the microscopic level (i.e., the Boolean field) has periodicity two in x_4 and the collision rules are identical at any two nodes differing only by their x_4 coordinates (e.g., fully deterministic rules, or rules changing randomly only with the first three coordinates), it then follows that the periodicity two is preserved at later times. For such solutions, it is sufficient to store the

[5] This appears superfluous for model FCHC-3.

states pertaining to two classes of nodes: those having $x_4 = 0$ and those having $x_4 = 1$. In four-dimensional space, these nodes form a staggered set, but they can be uniquely represented by their projections onto R^3, i.e., by the triplets (x_1, x_2, x_3) of signed integers with no restriction on their sum.

In actual implementations of this pseudo-4D model, additional obvious modifications are introduced, such as finiteness of the three-dimensional lattice and boundary conditions. For further details on actual machine implementations, see refs. 7–11.

8. RESULTS OF SIMULATIONS COMPARED TO BOLTZMANN PREDICTIONS

8.1. Kinematic Viscosity, Galilean Factor, Speed of Sound, and Reynolds Coefficient: Measurements

We measure the kinematic shear viscosity v and the Galilean factor $g(d)$ by the following method. A $256 \times 64 \times 64$ lattice is initialized with a uniform density d and a velocity $\mathbf{u} = (u_x, u_y, 0)$. The component u_x is uniform and positive. The component u_y is an x-dependent shear wave with wavenumber k and amplitude small compared to u_x. Linear theory indicates that the shear wave decays as e^{-vk^2t} and propagates in the x direction with a velocity $g(d)\,u_x$. We then let the lattice gas evolve and measure u_y at regularly spaced times by performing space averages over cells containing $1 \times 64 \times 64$ lattice nodes. A spatial Fourier transformation of u_y with respect to the x variable is performed at each output time. The time dependence of the complex amplitude of the Fourier mode with wavenumber k is extracted. Its argument and the logarithm of its modulus are then fitted to the linear time-evolution law predicted by theory, using a least squares method. From the slopes of these linear regressions we obtain respectively the Galilean factor $g(d)$ and the kinematic shear viscosity v.

We measure the speed of sound by the following method. A $256 \times 64 \times 64$ lattice is initialized with a suitable longitudinal (sound) wave of wavenumber k in the x direction. As before, we obtain the evolution of the Fourier modes of wavenumber k for the density fluctuations and the velocity u_x. From the ratio of the real parts of the complex amplitudes, we easily extract the speed of sound.[6]

We repeat each measure ten times with different random generator seeds, to evaluate the intrinsic noise level of the method. This leads to the error bars on subsequent figures.

[6] Viscous effects cannot be ignored if good accuracy is desired.

We now give the results for models FCHC-3 (Fig. 2), FCHC-7 (Fig. 3), and FCHC-8 (Fig. 4). In each figure, parts (a)–(d) correspond, respectively, to the Galilean factor $g(d)$, the speed of sound $c_s(d)$, the kinematic shear viscosity ν, and the Reynolds coefficient $R_*(d)$, which are plotted against the density d in a relevant interval. The solid curve is the theoretical value, based on the Boltzmann approximation; simulation results are shown with error bars.

We make some comments. For model FCHC-3, which satisfies semi-detailed balance, Boltzmann predictions for the Galilean factor and the speed of sound should be exact; they essentially provide a check on the numerical method. This remark does not apply to the kinematic viscosity, which is seen to be slightly higher than the Boltzmann value. As a consequence, the maximum value of the Reynolds coefficient $R_*^{\max}$ is about 6.4, somewhat lower than the Boltzmann prediction of 7.13.

For model FCHC-7, which violates semi-detailed balance, we observe discrepancies for the Galilean factor and the speed of sound, but not very large ones. The discrepancies are seen to be much more significant for the kinematic viscosity: the Boltzmann values change sign above $d_c \simeq 0.42$,

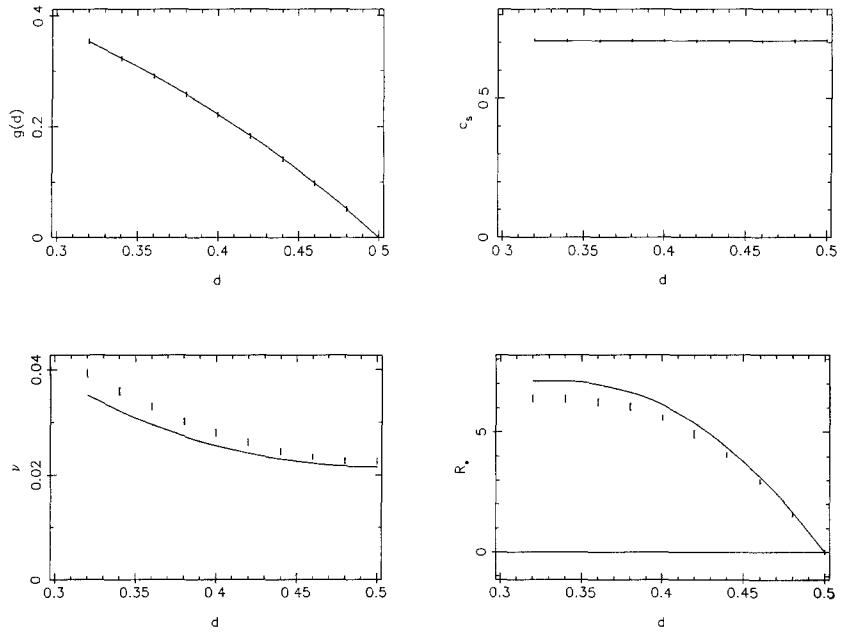

Fig. 2. (a) Galilean factor, (b) speed of sound, (c) kinematic shear viscosity, and (d) Reynolds coefficient for model FCHC-3. Solid curves: theoretical Boltzmann values. Error bars: numerical simulation results.

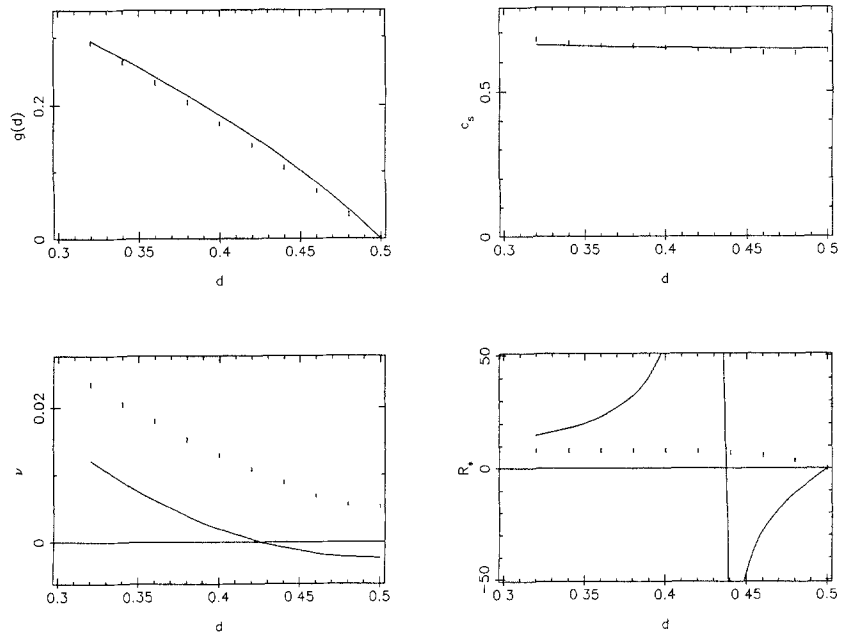

Fig. 3. Same as Fig. 2, but for model FCHC-7.

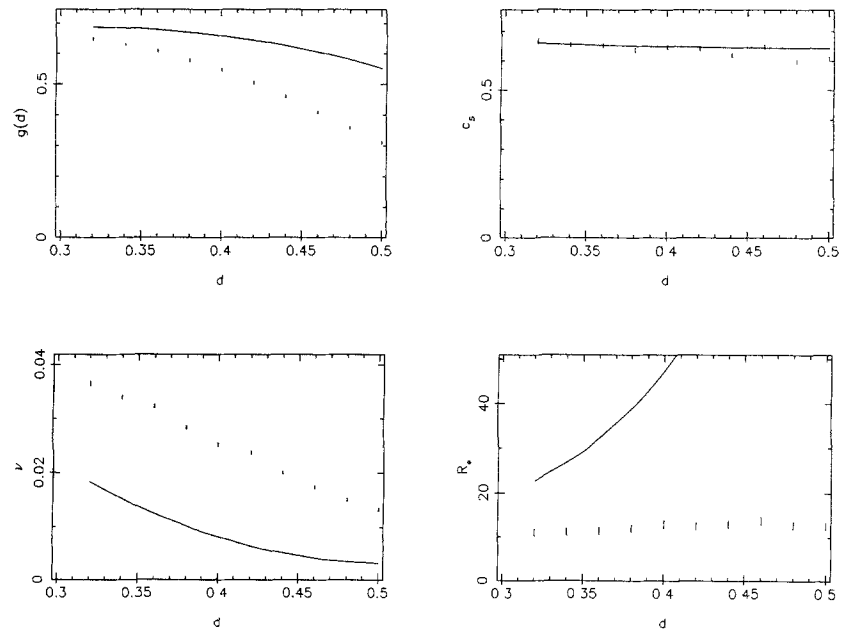

Fig. 4. Same as Fig. 2, but for model FCHC-8.

while the simulated values drop to a very low value of approximately 5×10^{-3}, but stay positive. As a consequence, the Boltzmann predictions for R_* are now completely off the mark. The largest achievable value is $R_*^{\max} \simeq 7.9$. Thus, only a marginal improvement has been achieved with respect to model FCHC-3.

For model FCHC-8, the Galilean factor is seen to be significantly lower than the Boltzmann values and the viscosity significantly higher. Both of these effects tend to reduce the Reynolds coefficient. Nevertheless, $R_*^{\max}$ is now about of 13.5, a noticeable improvement over previous implemented models. Further discussion of the results is found in Sections 9.1 and 9.2.

8.2. Measurements of Correlations for Basic Equilibria

We now report some properties of basic equilibria. For all cases discussed in Section 8, that is, for models FCHC-3, FCHC-7, and FCHC-8, we have checked that the basic equilibria are indeed obtained. More precisely, we observed that starting from a nonequilibrium state statistically uniform and uncorrelated, corresponding to a zero global velocity and a given global density, the average populations of the different velocities relax to steady values in a few time steps (less than 20).

We have measured the correlations for basic equilibria. We know that, with semi-detailed balance, equilibria are exactly factorized. Thus, there are no (single-time) correlations between particles pertaining to different nodes and/or velocities. Correlation coefficients between the Boolean variables n_i and n_j, corresponding to two velocities at the same node, may provide useful information about deviations from the Boltzmann approximation. The relevant correlations should then be measured just before collisions, since this is the quantity neglected by the Boltzmann approximation. We shall limit ourselves to basic (zero-velocity) equilibria.

Correlations are measured for various models and densities from simulations on a lattice 128×128 by letting the system relax to global equilibrium. Specifically, we define the correlation coefficient as $\mathscr{C}_{ij} = \mathrm{Cov}(n_i, n_j)/[\sigma(n_i)\,\sigma(n_j)]^{-1/2}$, where σ denotes a variance and Cov a covariance.

For the model FCHC-3, where no correlations are predicted, the measured correlation coefficient is indeed essentially noise, at a level of less than 7×10^{-3} for any pair of velocities and for the explored densities ranging from 0.32 to 0.50.

For the model FCHC-7, semi-detailed balance does not hold and substantial correlations are observed. For $d = 0.5$ the absolute value of the correlation coefficient is between 0.05 and 0.22, depending on the pair of

velocities considered. At lower densities, correlations drop, as expected: the maximum correlation for $d=0.32$ is 0.11. Furthermore, correlations display some anisotropy. If strict G-invariance were to hold, the correlation coefficient $\mathscr{C}_{ij}$ should depend only on the angle θ_{ij} between the two velocities $\mathbf{c}_i$ and $\mathbf{c}_j$. Actually, we find that for $\theta=\pi/2$, the correlation coefficient depends on the fourth component of the velocities. For $d=0.5$ three different sets of values are obtained near -0.11, -0.08, and -0.22. This seems due to peculiarities of the pseudo-4D implementation (see Section 9.2). No significant anisotropies are found for the values 0, $\pi/3$, $2\pi/3$, and π of the angle θ.

Similar results hold for model FCHC-8. The maximum correlation is about -0.23 for $d=0.50$.

We observe that the correlation coefficients between rest particles and moving particles, and between two rest particles are both at the noise level.

9. CONCLUSIONS AND DISCUSSIONS

9.1. Summary of Results

We have studied a class of extended FCHC lattice gas models comprising an arbitrary number of rest particles and the most general local collision rules consistent with the basic conservation laws of mass and momentum.

The study comprises two main parts. The first part (Sections 2–6) is mostly theoretical. We used the Boltzmann approximation to obtain the Galilean factor, the speed of sound, the kinematic viscosity, and the Reynolds coefficient. We then performed computer-assisted (but exact) optimizations to find those collision rules possessing the lowest viscosity. The second part (Sections 7 and 8) is about implementation of some of the optimal models suggested by the Boltzmann approximation. We showed in detail how to construct collision lookup tables for efficient implementation on machines with a very large memory. We then performed simulations to extract the "true" values of the transport coefficients.

Let us now consider the results. The optimal Boltzmann viscosity has been found to become negative in a range of values of the density near $d=1/2$ as soon as there is more than one rest particle (see Fig. 1). This result may seem academic in view of the simulations reported in Section 8.1, which indicate that the lowest value found for the true viscosity (obtained for model FCHC-7) is positive and around 5×10^{-3}. The Boltzmann result is nevertheless significant in its own right. Indeed, in principle, lattice gas models can be constructed which obey exactly the Boltzmann approximation. They are obtained by taking the large-N limit of

a stack of N FCHC models with suitable random couplings. (An example for $N=2$ is given in the next section.)

In a context where all microscopic constants (density, particle speed, lattice constant) are order one, it may be surprising to find that the kinematic viscosity can be very small compared to one. Indeed, in a *free* gas, i.e., not constrained by a lattice, this would be unlikely. Here, however, this constraint introduces an element of order in the lattice gas which invalidates the usual picture for (classical) gases. Technically, lattice gases are known to possess a "collision viscosity" (collision dependent), which is order one when the density is order one, and a "propagation viscosity," also order one, but negative, and which stems only from particle propagation.[3,13] In our optimal models the two viscosities almost (or exactly) cancel each other by suitable fine tuning of the collision rules.

When the viscosity goes through zero, a phase transition is likely to take place, leading to the appearance of some large-scale organization, as observed, for example, in ref. 16. Even before the viscosity goes negative, when it becomes too small, new terms, not present in the Navier–Stokes equations, become relevant; for example, linear terms involving four space derivatives.[7] It is conceivable that the modified Navier–Stokes equations remain valid beyond the phase transition. Such questions will not be discussed further, since they are too speculative as long as we do not possess a three-dimensional implementable model with negative viscosity.

Next, we examine the results obtained by measuring the true transport coefficient of various FCHC models. Table III, an extended version of Table I, summarizes all the salient qualitative and quantitative features of the FCHC models so far studied by our group. A figure is given in the column "$R_*^{\max}$ measured" only when the corresponding model has been implemented (the reference then appears in boldface). d_* is the value of the (reduced) density at which the highest Boltzmann-based value of $R_*^{\max}$ is obtained. Parenthetical values are somewhat improper, since the viscosity can go through zero.

An interesting measure of the actual progress made in three-dimensional machine implementations is obtained by computing an effective speed

$$S_* = S(R_*^{\max})^4 \tag{85}$$

where S is the speed measured in node updates per second (in two-dimensional simulations, the fourth power should be replaced by a third power). The CPU time needed to simulate a three-dimensional flow of given

[7] Three space derivatives are ruled out if the collision matrix is parity invariant, that is, invariant under simultaneous reversal of all input and output velocities.

Table III. Main Properties of Various FCHC Models

Name	Collision rules	Optimization of v	Rest particles	Semi-detailed balance	Optimization of $g(d)$	d_*	R_*^{max} Boltzmann	R_*^{max} measured	Reference
FCHC-1	Algorithm	No	0	Yes	No	0.17	2.00	2.0	8, **9**
FCHC-2	Table	Approximate	0	Yes	No	0.32	6.44	—	10
FCHC-3	Table	Approximate	0	Yes	No	0.33	7.13	6.4	**7**, 10, **11**
FCHC-4	Table	Exact	0	Yes	No	0.33	7.57	—	10
FCHC-5	Table	Exact	3	Yes	No	0.38	10.71	—	10
FCHC-6	Table	Exact	0	No	No	0.42	17.2	—	12
FCHC-7	Table	Exact	3	No	No	(0.42)	(∞)	7.9	This work
FCHC-8	Table	Exact	3	No	Yes	0.50	99.7	13.5	This work

geometry at a given Reynolds number for a given number of large eddy-turnover times is inversely proportional to S_*. (We assume that no other physical effects are added, such as surface tension, combustion, or porosity.) For FCHC models 1, 3, 7, and 8, the values of S_* are, respectively, 8×10^6, 5×10^{10}, 11.7×10^{10}, and 10^{12}. We did not include these data in our table because they are somewhat misleading if not put in proper context: for example, our earliest model was only meant to validate the FCHC approach and had a rather low speed of 5×10^5 node updates per second (compared to about 3×10^7 for the later ones). Still, the effective speed factor should be useful in comparing two designs, say A and B, for special-purpose machines. If design B allows ten times more parallelism, and thereby a tenfold increase in the speed S, but at the cost of a drop of a factor two in the Reynolds coefficient, then design A is preferable for the simulation of three-dimensional incompressible flows.

9.2. Possible Improvements

The hunt for larger values of the Reynolds coefficient is still on. As we have seen, the existence of correlations between the input velocities, and the resultant invalidation of the Boltzmann approximation, appears to be responsible for the relatively limited improvements obtained with the present models. An immediate objective is therefore to try to understand how these correlations are created, and then, if possible, to invent appropriate remedies in order to decrease the size of the correlations or even to reverse their sign.

One possible explanation for the rather large observed correlations is as follows. In a fully four-dimensional FCHC simulation, correlations created by the collisions at time t can contaminate the input to another collision only after two time-steps. As a result, the effect should be rather diluted. However, all our simulations use the pseudo-4D model in which nodes of the four-dimensional lattice are identified when their x_4 coordinates differ by a multiple of two (Section 7.3). Consider two particles coming out of the same node with velocities which differ only by the sign of the fourth coordinate, for instance $\mathbf{c}_i = (1, 0, 0, 1)$ and $\mathbf{c}_j = (1, 0, 0, -1)$. Because of the peculiar geometry of the simulation, these two particles will in effect get to the same node in just one time-step. Correlations between such particles at time t, generated by violation of semi-detailed balance, will be present at time $t+1$ in the input states and thus modify the viscosity. A simple heuristic reasoning indicates that this effect should add a positive contribution to the viscosity compared to the Boltzmann-based prediction and should also explain the strong negative correlations reported in Section 8.2.

A possible remedy is to use a lattice which is somewhat thicker in the fourth dimension. Reduction of correlations can also be achieved by random coupling of two FCHC models, say FCHCu and FCHCd (u and d for "up" and "down"). Let their respective Boolean fields be $n_{Iu}(t, \mathbf{x})$ and $n_{Id}(t, \mathbf{x})$. Just before collision, random permutations of bits are made: at each node and for each velocity I, the bits n_{Iu} and n_{Id} are interchanged with probability 1/2. In practice, pseudorandom choices can be used.

We are exploring the above ideas for further improvements of the Reynolds coefficient.

9.3. Too Much vs. Too Little Resolution

In a fluid made of real molecules, there is usually a wide separation of scales between the mean free path and the smallest hydrodynamic scale. For example, atmospheric turbulence in the planetary boundary layer has a separation of scales of at least four orders of magnitude. The separation of scales is an increasing function of the Reynolds number when the Mach number is held fixed.[19]

Similarly, it was argued by Orszag and Yakhot[15] that, when the Reynolds number is increased in a lattice gas simulation, increasing waste of resolution results, i.e., an increasing fraction of the stored data contains useless microscopic information. They assumed that the kinematic viscosity of the lattice gas would be of order unity in lattice units. In view of the results presented in the present paper (and also of further expected progress in construction of low-viscosity models), it becomes necessary to reexamine the waste-of-resolution argument. We shall here limit ourselves to flow governed by the incompressible Navier–Stokes equations. For the case of Rayleigh–Bénard convection, see ref. 20.

We denote by l_d, the dissipation scale, the smallest excited scale in the flow. We denote by l_0 the integral scale and by M the Mach number of the flow. Everything is in lattice units. The Reynolds number R is given by (51). The best available information (no full theory) on turbulent flows indicates that for large R

$$\frac{l_d}{l_0} \simeq CR^{-m} \tag{86}$$

where C is a numerical constant and m an exponent which depends on the type of flow. For two-dimensional isotropic turbulence, $m = 1/2$. For three-dimensional isotrpic turbulence, $m = 3/4$. For three-dimensional turbulence near a wall m is somewhere between 3/4 and 1. From (51) and (86), it follows that

$$l_d \simeq C(MR_*)^{-1} R^{1-m} \tag{87}$$

where R_* is the Reynolds coefficient. For fixed Mach number and Reynolds coefficient and any exponent $m < 1$, the dissipation scale tends to infinity with the Reynolds number. Since the dissipation scale is measured in lattice units, this indicates increasing *waste* of resolution at high Reynolds number.

Now, let us hold the Mach number and the Reynolds number fixed, and consider a sequence of models with increasing Reynolds coefficients used to simulate the flow. Both the integral scale and the dissipation scale will decrease (as R_*^{-1}). The consequences are twofold.

First, consider the computational work needed to simulate the flow for a given number of large eddy turnover times. It scales like R_*^{-3} in two dimensions and R_*^{-4} in three dimensions. Thus, as already stressed, increasing R_* is computationally very advantageous. To take an extreme example, compare the same two-dimensional flow computed first with the original FHP-I rule[3] and then with the optimized FCHC-8 model (projected down to two dimensions). The efficiency gain (measured by the ratio of the necessary node updates) is $(13.5/0.387)^3 \simeq 42{,}000$. A comparison of the computational work required for floating-point methods and lattice gas methods has been made by Zaleski.[20]

A second consequence of increasing R_* is that the dissipation scale may become smaller than the size of the averaging cells needed to extract hydrodynamic signals from microscopic noise (say, 4–8 lattice constants[11]). We then lose the hydrodynamic information about the smallest scales, but the simulation is still faithfully solving the Navier–Stokes equations, as long as the dissipation scale is larger than a few lattice constants. If we then further increase R_*, so that the dissipation scale computed from (87) would become less than one lattice constant, the continuum Navier–Stokes approximation will break down at small scales. The equivalent action in a traditional floating-point calculation, i.e., the excessive lowering of the viscosity, leads to disaster: either the solution will blow up or it will go to hydrodynamically unphysical states, such as equipartition of energy among all spatial Fourier modes. In lattice gases, such disaster seems ruled out, because the model stays exactly realizable as a system of interacting Boolean particles.[8] Large-scale behavior will still be governed by the Navier–Stokes equations. But it may not be faithfully represented (for the given Reynolds number), since the largest and the smallest scales are interdependent (in a way mostly unknown). In the language of computational fluid dynamics, modifications of the Navier–Stokes equations at small scales, with the purpose to simulate flows at Reynolds numbers too

[8] The same holds for methods using the lattice Boltzmann equation,[21,22] provided no simplifying expansion is used which could violate realizability.

large for the mesh, are known as *sub-grid-scale models.* Without theoretical understanding of small-scale motion, this remains an empirical field, where the merits of a given procedure can be estimated only by comparisons with experiments (or fully resolved simulations, when available).

In refs. 7 and 11 a lattice gas simulation of three-dimensional flow around a circular plate has been reported. It uses model FCHC-3 with $R_*^{\max} = 6.4$ and a Reynolds number of about 200. It appears that the very smallest structures in the boundary layer near the plate are only marginally resolved.[23] We are thus at the borderline of having *too little resolution.* An assessment of lattice gas simulations as sub-grid-scale models may become necessary.

ACKNOWLEDGMENTS

We thank D. d'Humières for useful discussions. CRAY-2 resources have been provided by the Centre de Calcul Vectoriel pour la Recherche. This work has been supported by DRET (88/1450), the EEC (SC1-0212-C), and Los Alamos (9-L38-3634R). One of us (B. D.) received partial support from an Amelia Earhart fellowship of the Zonta foundation.

REFERENCES

1. U. Frisch, B. Hasslacher, and Y. Pomeau, Lattice gas automata for the Navier–Stokes equation, *Phys. Rev. Lett.* **56**:1505–1508 (1986).
2. J. Hardy, Y. Pomeau, and O. de Pazzis, Time evolution of a two-dimensional model system. I. Invariant states and time correlation functions, *J. Math. Phys.* **14**:1746–1759 (1973).
3. U. Frisch, D. d'Humières, B. Hasslacher, P. Lallemand, Y. Pomeau, and J.-P. Rivet, Lattice gas hydrodynamics in two and three dimensions, *Complex Systems* **1**:649–707 (1987) [reprinted in *Lecture Notes on Turbulence*, I. R. Herring and J. C. McWilliams, eds. (World Scientific, 1989), pp. 297–371].
4. S. Wolfram, Cellular automaton fluids 1: Basic theory, *J. Stat. Phys.* **45**:471–526 (1986).
5. D. d'Humières and P. Lallemand, Numerical simulations of hydrodynamics with lattice gas automata in two dimensions, *Complex Systems* **2**:599–632 (1987).
6. D. d'Humières, P. Lallemand, and U. Frisch, Lattice gas models for 3-D hydrodynamics, *Europhys. Lett.* **2**:291–297 (1986).
7. J.-P. Rivet, M. Hénon, U. Frisch, and D. d'Humières, Simulating fully three-dimensional external flow by lattice gas methods, *Europhys. Lett.* **7**:231–236 (1988).
8. M. Hénon, Isometric collision rules for the four-dimensional FCHC lattice gas, *Complex Systems* **1**:475–494 (1987).
9. J.-P. Rivet, Simulation d'écoulements tri-dimensionnels par la méthode des gaz sur réseaux: premiers résultats, *C. R. Acad. Sci. Paris II* **305**:751–756 (1987).
10. M. Hénon, Optimization of collision rules in the FCHC lattice gas, and addition of rest particles, in *Discrete Kinetic Theory, Lattice Gas Dynamics and Foundations of Hydrodynamics*, R. Monaco, ed. (World Scientific, 1989), pp. 146–159.

11. J.-P. Rivet, Hydrodynamique par la méthode des gaz sur réseaux, Thèse, Université de Nice (1988).
12. B. Dubrulle, Method of computation of the Reynolds number for two models of lattice gas involving violation of semi-detailed balance, *Complex Systems* **2**:577–609 (1988).
13. M. Hénon, Viscosity of a lattice gas, *Complex Systems* **1**:763–789 (1987).
14. J. A. Somers and P. C. Rem, The construction of efficient collision tables for fluid flow computations with cellular automata, in *Cellular Automata and the Modelling of Complex Systems* (Springer, 1989).
15. S. A. Orszag and V. Yakhot, Reynolds number scaling of cellular automaton hydrodynamics, *Phys. Rev. Lett.* **56**:1691–1693 (1986).
16. D. H. Rothman, Negative-viscosity lattice gases, *J. Stat. Phys.* **56**:517–524 (1989).
17. H. Chen, S. Chen, G. D. Doolen, Y. C. Lee, and H. Rose, Multithermodynamic phase lattice gas automata incorporating interparticle potentials, *Phys. Rev. A* **40**:2850–2853 (1989).
18. C. H. Papadimitriou and K. Steiglitz, *Combinatorial Optimization: Algorithms and Complexity* (Prentice-Hall, Englewood Cliffs, New Jersey, 1982).
19. U. Frisch, Où en est la turbulence développée?, *Phys. Scripta* **9**:137–146 (1985).
20. S. Zaleski, Weakly compressible fluid simulations at high Reynolds numbers, in *Discrete Kinetic Theory, Lattice Gas Dynamics and Foundations of Hydrodynamics*, R. Monaco, ed. (World Scientific, 1989), pp. 384–394.
21. G. R. MacNamara and G. Zanetti, Use of the Boltzmann equation to simulate lattice-gas automata, *Phys. Rev. Lett.* **61**:2332–2335 (1988).
22. F. J. Higuera, Lattice gas simulation based on the Boltzmann equation, in *Discrete Kinetic Theory, Lattice Gas Dynamics and Foundations of Hydrodynamics*, R. Monaco, ed. (World Scientific, 1989), pp. 162–177.
23. A. Patera, Private communication (1988).